Materials Science-Poland, 33(4), 2015, pp. 742-750
http://www.materialsscience.pwr.wroc.pl/
DOI: 10.1515/msp-2015-0087

DE GRUYTER OPEN

Impact of incorporation of chromium on electrochemical properties of $LiFePO_4$/C for Li-ion batteries

AMOL NAIK[1], JIAN ZHOU[1*], CHAO GAO[1], GUIZHEN LIU[1], LIN WANG[2]

[1]State Key Laboratory of Advanced Technology for Materials Synthesis and Processing, Wuhan University of Technology, Wuhan 430070, P. R. China

[2]Key Laboratory of Fiber Optic Sensing Technology and Information Processing, Ministry of Education, Wuhan University of Technology, Wuhan 430070, P. R. China

$LiFe_{0.95}Cr_{0.05}PO_4$/C was successfully synthesized by one-step solid-state reaction using a single mode microwave reactor. The effect of incorporation of chromium on $LiFePO_4$ lattice parameters was systematically investigated by X-ray diffraction. Surface analysis was done by scanning electron microscopy and transmission electron microscopy. The ratio of amorphous to graphitic carbon was determined from Raman spectroscopic data. The influence of chromium incorporation on electrochemical properties was studied by recording charge/discharge cycles combined with electrochemical impedance spectroscopy (EIS) and cyclic voltammetry. It was found that Cr incorporation significantly enhanced the electrochemical performance of $LiFePO_4$ at all current densities up to 10 C. $LiFe_{0.95}Cr_{0.05}PO_4$/C prepared exhibited the best performance with an initial specific discharge capacity of 157.7, 144.8, 138.3, 131.0, 124.1 and 111.1 $mAh{\cdot}g^{-1}$ at 0.1 C, 0.5 C, 1.0 C, 2.0 C, 5 C and 10 C, respectively. The doped sample displayed excellent capacity retention, which was substantially superior than that of pristine $LiFePO_4$/C at a higher current rate.

Keywords: *one step solid state reaction; chromium incorporation; $LiFe_{0.95}Cr_{0.05}PO_4$/C; higher current densities*

© Wroclaw University of Technology.

1. Introduction

Recently, the evolving applications for lithium-ion battery technology in electrical energy storage systems for smart grids that are powered by traditional energy sources, like coal, as well as intermittent renewable energy sources, like solar and wind ones, have been attracting more and more attention [1]. Owing to the fact that storage of electrical energy will be far more important in this century than it was in the last decade, there is the need for further enhancement in energy and power density, cycle life, and safety performance of lithium-ion battery, to meet future challenges of energy storage [2]. Olivines have been the focus of rigorous study, since the original work of Padhi et al. [3] showed their redox behaviour. Though olivine $LiFePO_4$ is considered as a viable option for Li-ion battery, it suffers from two major hindrances, one is the low electronic conductivity (10^{-7} to 10^{-9} S/cm), which leads to its poor rate capability; the other is the slow lithium-ion diffusion across the $LiFePO_4/FePO_4$ boundary [4, 5]. To eliminate these two major impediments of $LiFePO_4$, numerous approaches, such as conductive additive coating [6, 7], super valence cation doping [8], and minimizing particle size by different synthesis routes [9–11], have been reported. Fe-site doping is considered to be an effective way to improve the rate performance of $LiFePO_4$, resulting from the increased ionic mobility and diffusion coefficient.

The present study is focused on enhancement of electrochemical properties of $LiFePO_4$ by partial substitution of Fe^{2+} by Cr^{3+}. The effects on conductivity of NASICON on substitution of Cr^{3+} have been investigated by several workers [12–14]. Not much work related to substitution of Cr^{3+} in $LiFePO_4$, except few ones, have been carried out [15, 16]. Ying et al. [15]

*E-mail: jianzhou@whut.edu.cn

prepared spherical $Li_{0.97}Cr_{0.01}FePO_4$/C composites by controlled crystallization-carbothermal reduction method. They have demonstrated that at 0.005, 0.05, 0.1, 0.25 and 1 C current densities, $Li_{0.97}Cr_{0.01}FePO_4$/C can achieve the initial discharge capacity of 163, 151, 142, 131 and 110 $mAh \cdot g^{-1}$, respectively, and also showed excellent cycling performance due to the enhanced electronic conductivity caused by the Cr^{3+} substitution and carbon coating. The tap density of the spherical $Li_{0.97}Cr_{0.01}FePO_4$/C powders was as high as 1.8 g cm^{-3}, which is significantly higher than that reported for non-spherical $LiFePO_4$ powders. They claimed that the high-density spherical $Li_{0.97}Cr_{0.01}FePO_4$/C cathode materials can provide significant incentive for battery manufactures to consider them as very promising candidates to be utilized in the lithium-ion batteries with high power density. The method suggested by Ying et al., involved multiple steps and long duration, however, the performance of the material at higher current densities has not been reported. Park et al. [16] successfully synthesized $LiFe_{0.97}Cr_{0.03}PO_4$/C by heating a solid mixture of Li_2CO_3, $FeC_2O_4 \cdot 2H_2O$, $(NH_4)H_2 \cdot PO_4$ and $(CH_3CO_2)_7Cr_3(OH)_2$. Diffusion coefficient of lithium (D_{Li}) was determined by implementing cyclic voltammetry and electrochemical impedance spectroscopy. Park et al. [16] further stated that the low diffusivity of the $LiFePO_4$/C leads to the considerable capacity decline at high discharge rates, while high diffusivity of the $LiFe_{0.97}Cr_{0.03}PO_4$/C maintains the initial capacity at high C-rates. But the performance of their material was not much impressive; also they measured stability only for five cycles at each current density. In addition, the method adopted required heating at 750 °C in Ar + 5 % H_2 atmospheres for 10 h. Inspired by this work, our investigation aimed to design a suitable and fast synthesis route for chromium doped and porous $LiFePO_4$ using a single mode microwave reactor. In our recent work we have shown how a presence of pores can improve the electrochemical properties of $LiFePO_4$ [17]. Hence, in this manuscript we report the synthesis of porous $LiFe_{0.95}Cr_{0.05}PO_4$/C with improved specific capacity even at low current densities, on account of an increase in contact area of active material with electrolyte. $Fe_2(CO)_9$ was used as an iron source, which produced CO gas on decomposition, whose evolution resulted in porous $LiFe_{0.95}Cr_{0.05}PO_4$/C. Another advantage was that the evolved CO gas maintained inert atmosphere within the sample bulk, which prevented oxidation of Fe^{2+} ions. Therefore, there was no requirement of injecting inert gas in the reactor separately. The detailed comparative studies on electrochemical properties of as prepared $LiFe_{0.95}Cr_{0.05}PO_4$/C with bare and carbon coated $LiFePO_4$ are described in this research article.

2. Experimental

2.1. Materials

Lithium acetate ($LiOOCCH_3 \cdot 2H_2O$), ammonium dihydrogen phosphate ($NH_4H_2PO_4$), chromium nitrate ($Cr(NO_3)_3 \cdot 9H_2O$) and citric acid were supplied from SCR, Shanghai, China; di-iron nonacarbonyl ($Fe_2(CO)_9$) was provided from Jiangsu Tianyi Ultra-Fine Metal Powder Co. Ltd, Jiangsu, China. All chemicals were analytical grade and used without further purification.

2.2. Synthesis of $LiFePO_4$/C

$LiFe_{0.95}Cr_{0.05}PO_4$/C was synthesized by the following solid state microwave path. In a typical synthesis, a stoichiometric amounts of $NH_4H_2PO_4$ and $Fe_2(CO)_9$ were mixed in an agate mortar with a pestle for 30 minutes. The homogeneous mixture obtained was heated in an oven at 80 °C for 10 min and subsequently ground thoroughly with $LiOOCCH_3 \cdot 2H_2O$, $Cr(NO_3)_3 \cdot 9H_2O$ and citric acid for another 30 min. The mixture obtained was ball milled for 15 h in ethanol and dried at 70 °C. The free flowing powder obtained was compressed (12 MPa) to pellets and heated in a sealed quartz crucible. Similar procedure was followed to synthesize bare $LiFePO_4$ as well as $LiFePO_4$/C composite. Microwave irradiation of all the mixtures was performed in a specially designed single mode microwave furnace at 2.45 GHz and 136 W for 8 min.

2.3. Characterization of synthesized $LiFePO_4/C$

The crystalline structure of the pristine and Cr-doped sample was analyzed by powder X-ray diffraction (PANalytical X'Pert Pro) and performed using CuK_α radiation ($\lambda = 1.54056$ Å). The data were collected from 10 to 80° in 2θ range, with a step size of 0.017 and 1.0 s per step. The microstructure of the powder samples was observed with a scanning electron microscope (JSM-5610LV) and a transmission electron microscope (TEM), (JEM-2010), whereas the surface analysis of the compressed pellets was done by Hitachi field-emission scanning electron microscope (FE-SEM S-4800). The properties of porous composite in the 4 to 200 nm range were determined by nitrogen adsorption at 77 K using an ASAP 2000 instrument from Micromeritics. A sample of a mass around 200 mg was loosely pressed into a pellet and then evacuated at 573 K under 0.1 Pa prior adsorption. The Raman spectroscopic analysis (INVIA RENISHAW laser Raman spectroscope) was performed with a system utilizing 632.5 nm incident radiation and a 50× aperture (N.A. = 0.75), resulting approximately in a sampling cross section of 2 μm in diameter.

2.4. Electrochemical measurements

A cathode working electrode for electrochemical testing was prepared by mixing the product with acetylene black and 5 % solution of polytetrafluoroethylene (PTFE) in water, with a weight ratio of 80:10:10. The slurry prepared in isopropyl alcohol was coated on a thin aluminium sheet and dried in a vacuum oven at 120 °C for 24 h. 2025 type coin cells were assembled using lithium foil as an anode and 1 M solution of $LiPF_6$ in a mixture of ethylene carbonate and dimethylene carbonate (1:1 v/v) as an electrolyte in an argon-filled glove box at room temperature. The two electrodes in the cell were held apart by a separator (Celgard No. 2402). Charge-discharge characteristics of the sample were cycled between 2.7 to 4.2 V using battery test system (LAND CT2001A) at the ambient temperature. Cyclic voltammetry (CV) and electrochemical impendence spectroscopic (EIS) measurements were performed on Auto Potentiostat30 system. The amplitude of the AC signal was 5 mV over the frequency range between 0.01 Hz and 100 kHz.

3. Results and discussion

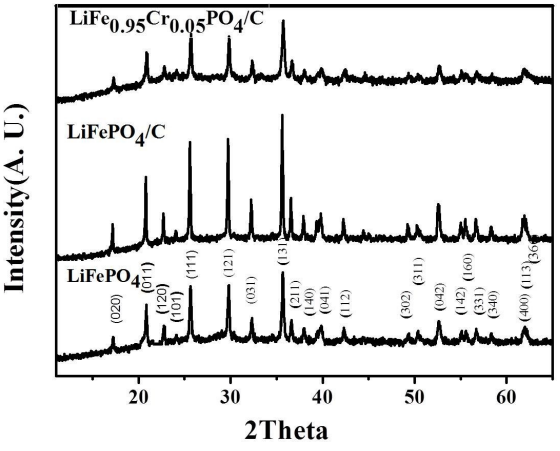

Fig. 1. XRD patterns of as prepared samples.

Fig. 1 shows XRD patterns of the as-prepared, bare $LiFePO_4$, $LiFePO_4/C$ and $LiFe_{0.95}Cr_{0.05}PO_4/C$ composites. It is found that Cr-doped $LiFePO_4/C$ has well crystallized in orthorhombic structure as in the pristine sample, without any unexpected phases, such as Fe_2P or Cr-containing compounds [18]. All diffraction peaks match well with the standard data for pure $LiFePO_4$ phase (PDF-40-1499). This suggests that the olivine structure of $LiFePO_4$ was well preserved during the preparation process.

The data in Table 1 infer that compared with $LiFePO_4/C$, both unit parameters and unit cell volume of $LiFe_{0.95}Cr_{0.05}PO_4/C$ decreased after Cr substitution, which can be ascribed to the substitution of Fe^{2+} ions by smaller size Cr^{3+} ions. ICP analysis of the $LiFe_{0.95}Cr_{0.05}PO_4/C$ indicates that the real contents of Li, Fe, and Cr in the sample are 1.085, 0.951 and 0.0503, respectively, (higher value of Li is due to multiplication of error, since the sample preparation for ICP measure involved multiple dilutions), which are in a close agreement with expected values. EDS results in Fig. 2 further

Table 1. Calculated lattice parameters of $LiFePO_4$/C and $LiFe_{0.95}Cr_{0.05}PO_4$/C.

Lattice Parameter	Samples		
	$LiFePO_4$	$LiFePO_4$/C	$LiFe_{0.95}Cr_{0.05}PO_4$/C
a (Å)	10.2946 ± 0.0002	10.3196 ± 0.0002	10.2586 ± 0.00018
b (Å)	5.9885 ± 0.0012	6.0102 ± 0.0011	5.9943 ± 0.0012
c (Å)	4.6861 ± 0.0003	4.6939 ± 0.0004	4.6800 ± 0.0029
Volume of unit cell ($Å^3$)	288.8943 ± 0.0014	291.1291 ± 0.0016	287.7878 ± 0.0013

confirm the successful substitution of chromium in the $LiFePO_4$ matrix.

Fig. 3a – 3c depict the typical SEM images of the as prepared $LiFe_{0.95}Cr_{0.05}PO_4$/C composite at different magnifications and Fig. 3d shows a SEM image for $LiFePO_4$/C. From the images it can be concluded that both the products consist of porous agglomerations (Fig. 3a). The pores are clearly noticeable in magnified images (Fig. 3b, 3c). FE-SEM pictures evidence that the porous agglomerations observed consist of non-uniform fine particles with the grain size of 25 to 100 nm. The particles size and uniform distribution of conducting carbon have been further confirmed by the TEM image (Fig. 4) of $LiFe_{0.95}Cr_{0.05}PO_4$/C. The total amount of carbon in the bare and substituted $LiFePO_4$ was estimated by thermogravimetry and it was found to be 2.65 and 2.63 %, respectively. The carbon coating provides highly conductive channel for electron transport among active $LiFePO_4$ particles, what enhances the electronic conductivity of the composites [19]. In addition, porosity in as synthesized material acts as a channel for Li^+ ion transportation during charging/discharging cycles. It also increases the surface contact between the electrolyte and active cathode material.

It is evidenced from the Fig. 3 that the as synthesized material consist of porous agglomerations of smaller particles. The formation of pores can be assigned to evolution of gases during the decomposition of $Fe_2(CO)_9$, which also takes care of prevention of oxidation of Fe^{2+}. The detailed discussion about the synthesis method has been reported in our recent publication [17]. The qualitative picture of pores and voids of different dimensions has been confirmed by a quantitative analysis, namely by the measurement of N_2 adsorption isotherms [20]. Detailed analysis showed that the average pore size is 80 to 110 nm in the macroporous range, and surface area is about 16 to 18 $m^2 \cdot g^{-1}$.

XPS analysis

X-ray photoelectron spectra exhibiting Cr, C and all the elements of $LiFePO_4$ are shown in Fig. 5. Li 1s is superimposed on the Fe 3p peak at about 56 eV [21]. The binding energy of P 2p, C 1s, and O 1s has been determined to be 133.7 eV, 284.9 eV, and 531.6 eV, respectively. A satellite peak close to the main Fe 2p3/2 peak (711.6 eV) at the higher binding energy of 716.3 eV is observed in the Cr-doped $LiFePO_4$/C samples. The appearance of this satellite peak is a characteristic feature of transition metal ions with partially filled d-orbitals [22]. Peaks of 2p1/2 and 2p3/2 for Cr^{4+} appear at 586.2 eV and 576.4 eV, while those for Cr^{3+} appear at 589.2 eV and 579.2 eV, respectively, further verifying the presence of Cr^{3+} in the obtained sample [23].

A non-stoichiometric cation ratio and Li-ion vacancies in $LiFePO_4$ may be induced in order to accommodate the introduced super valent Cr^{3+} ion. This, in turn, can facilitate lithium ion diffusion in these channels and, therefore, enhance the electrochemical performance.

Raman spectra

Fig. 6 shows the Raman spectra of $LiFePO_4$/C and $LiFe_{0.95}Cr_{0.05}PO_4$/C composites. The carbon layer on $LiFePO_4$ crystals makes it difficult to spot the details of the spectrum of olivine structure of $LiFePO_4$ due to weakening of the signals and overlapping of the spectral bands [24], except few peaks corresponding to PO_4^{3-} and

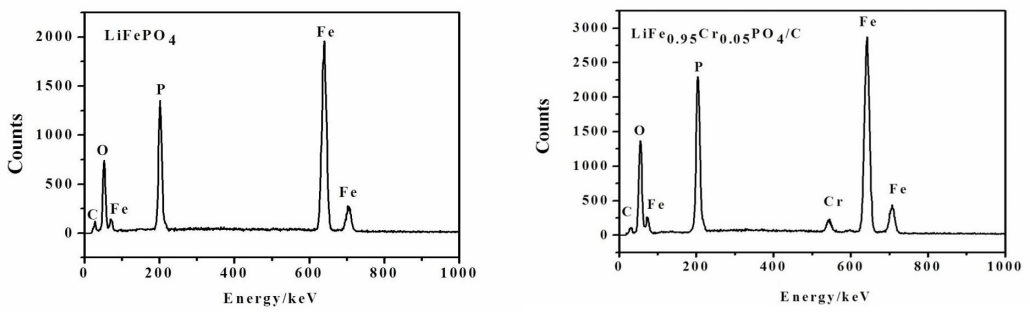

Fig. 2. EDS results of doped and undoped $LiFePO_4$.

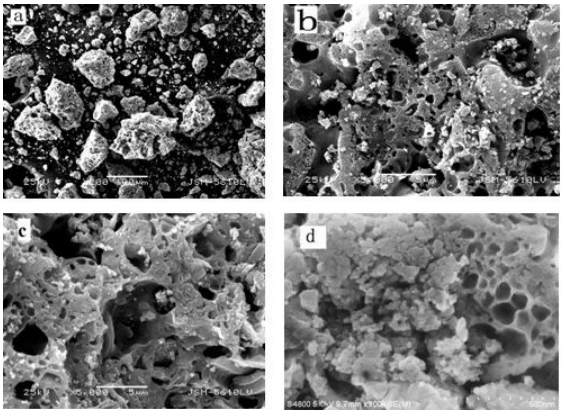

Fig. 3. (a), (b) SEM images of $LiFe_{0.95}Cr_{0.05}PO_4/C$ at different magnifications, (c) SEM images of $LiFePO_4/C$, (d) FE-SEM of $LiFe_{0.95}Cr_{0.05}PO_4/C$.

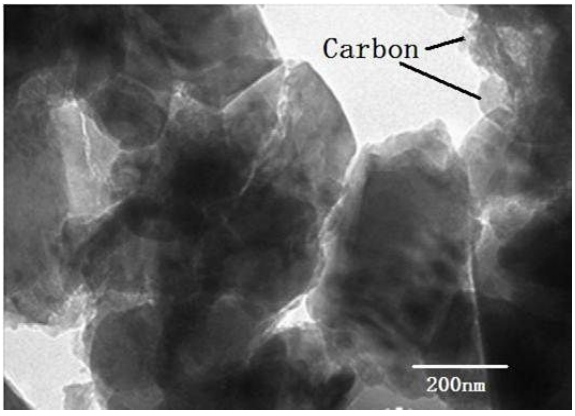

Fig. 4. TEM image of $LiFe_{0.95}Cr_{0.05}PO_4/C$.

Fe–O bonds. Two peaks at 1600 and 1336 cm^{-1} correspond to the G and D bands of carbon, respectively. The presence of D band infers the disorder induced in sp^2-bonded carbon, whereas the G band evidences in-plane vibration of sp^2 carbon atoms [25, 26]. However, D and G bands of $LiFePO_4/C$ and $LiFe_{0.95}Cr_{0.05}PO_4/C$ are observed at 1340 and 1581 as well as at 1344 and 1578, respectively. I_D/I_G value (the peak intensity ratio between 1336 and 1600 cm^{-1} peaks) generally provides useful information to compare the degree of crystallanity of various materials, i.e. the smaller the ratio, the higher the degree of carbon ordering in the material. For $LiFePO_4/C$, I_D/I_G ratio is 1.20, but for $LiFe_{0.95}Cr_{0.05}PO_4/C$ it has increased to 1.22. The I_D/I_G ratios for both the samples differ very marginally which indicates the shares of graphite realm in both the samples are almost the same. Hence, the enhancement of electrochemical performance of $LiFe_{0.95}Cr_{0.05}PO_4/C$ compared to $LiFePO_4/C$ is purely due to doping of chromium, as porosity is similar in both the samples (Fig. 3).

3.1. Electrochemical properties of synthesized $LiFePO_4$

To analyse the electrochemical properties of the $LiFe_{0.95}Cr_{0.05}PO_4/C$, cyclic voltamograms were collected as shown in Fig. 7. The voltage was in the range of 2.0 to 4.2 V vs. Li/Li^+. Fig. 7 shows the first three cycles recorded at a scan rate of 0.2 mV/s. There is only a single pair of peaks for each cycle, implying typical two phase reaction between $LiFePO_4$ and $FePO_4$ [27]. The redox peaks of the first cycles are located at 3.20 and 3.66 V, which corresponds to extraction and insertion of Li^+. The polarization, which was 0.46 V in the first cycle, decreased for succeeding two

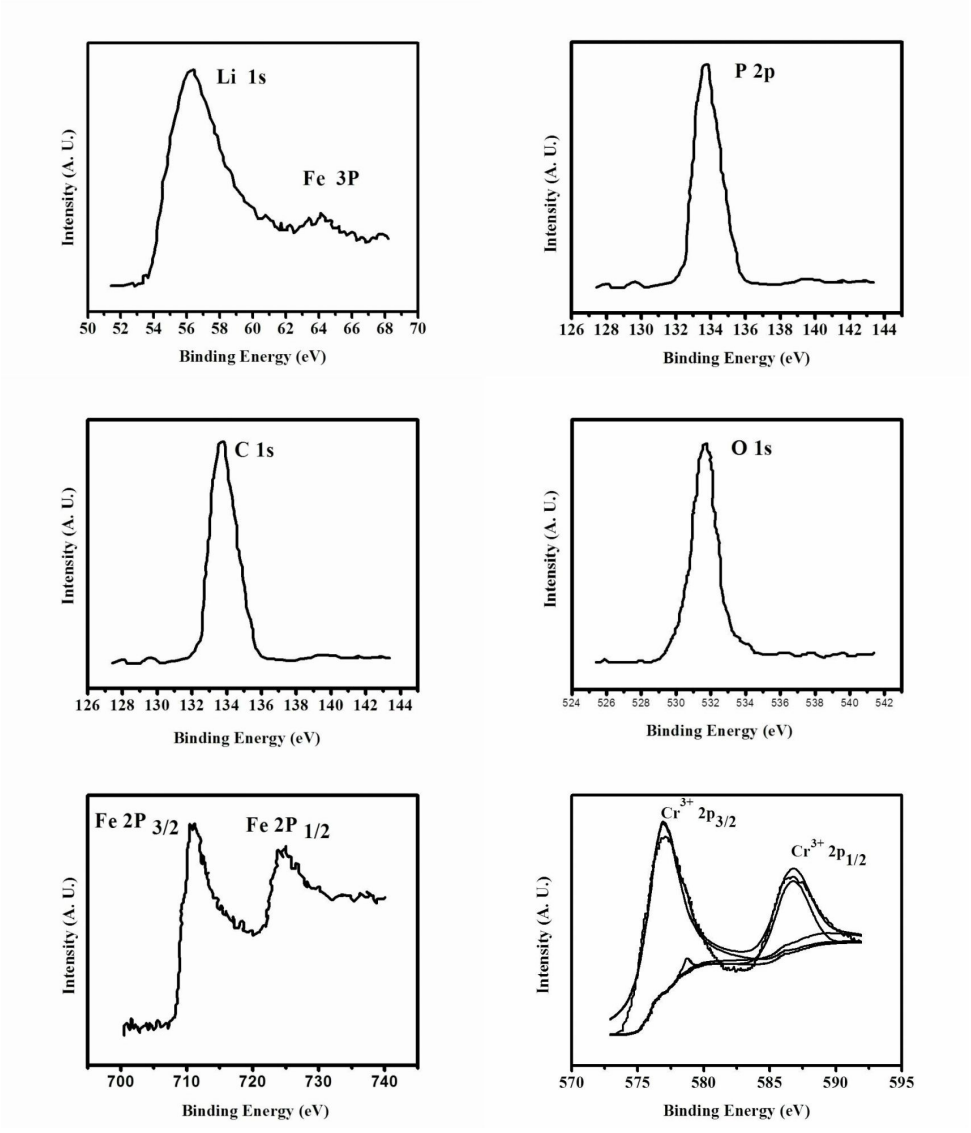

Fig. 5. XPS spectra of all elements in the Cr-doped $LiFePO_4$/C sample.

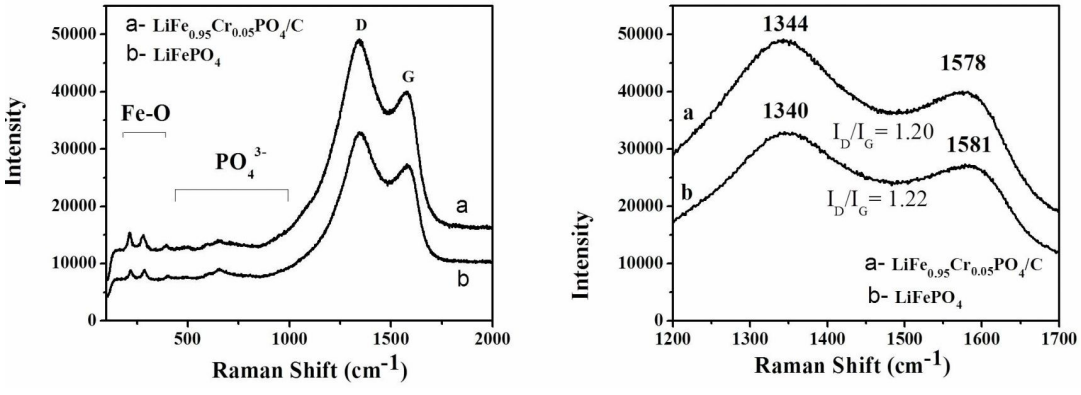

Fig. 6. Raman spectra of doped and undoped samples.

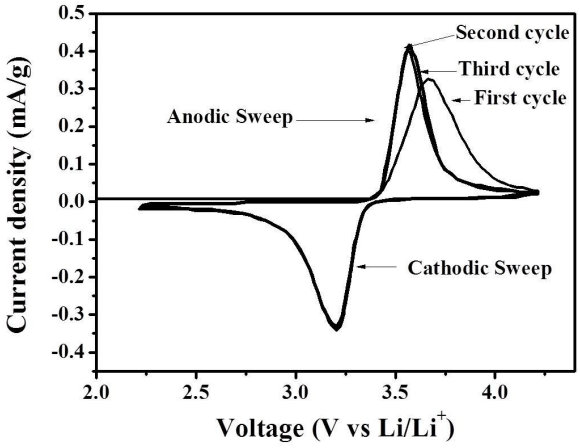

Fig. 7. Cyclic voltammograms of $LiFe_{0.95}Cr_{0.05}PO_4/C$.

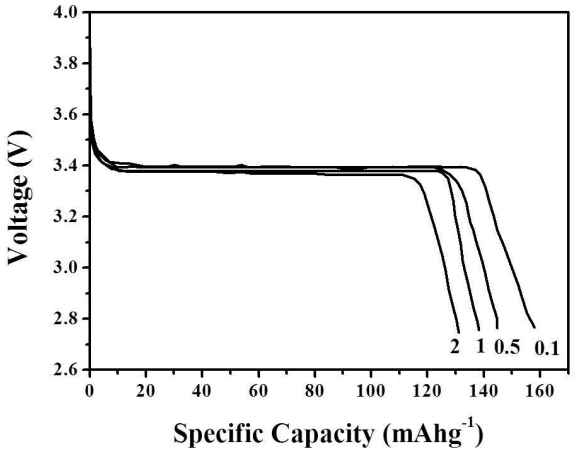

Fig. 9. First cycle discharge performance of $LiFe_{0.95}Cr_{0.05}PO_4/C$ at different current rates (0.1C to 2.0C).

cycles. After activation by the first redox cycle, the current peak of the following sets became sharper and higher. The curves of the second and third cycles are almost superimposed except a few regions, indicating that the electrochemical reversibility of $LiFe_{0.95}Cr_{0.05}PO_4/C$ was well established after the first cycle [28].

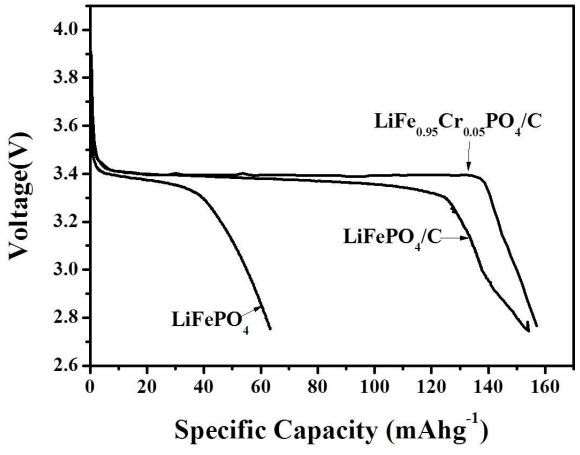

Fig. 8. Discharge curve of bare, carbon coated and Cr-doped $LiFePO_4/C$ cathodes at at 0.1 C current density.

Fig. 8 shows the comparative initial galvanostatic discharge curves of bare, carbon coated and Cr-doped $LiFePO_4/C$ cathodes, which were obtained at a current density of 0.1 C in the voltage range of 2.7 to 4.2 V (vs. Li/Li^+). There is no noticeable discharge plateau associated with the Cr^{3+}. This indicates that Fe^{2+}/Fe^{3+} is practically the only redox couple that contributes to the electrochemical reaction in the $LiFe_{0.95}Cr_{0.05}PO_4/C$ cathode. It is also found that $LiFe_{0.95}Cr_{0.05}PO_4/C$ exhibits the highest discharge capacities of 157.7 $mAh{\cdot}g^{-1}$, compared to 154.2 and 63.4 $mAh{\cdot}g^{-1}$ of $LiFePO_4/C$ and $LiFePO_4$, respectively, which is significantly higher than that reported by Park et al. [16]. Higher capacity suggests that the highest amount of Fe^{2+} in $LiFe_{0.95}Cr_{0.05}PO_4/C$ was electrochemically utilized at 0.1 C rate, indicating that the utilization of the Fe^{2+}/Fe^{3+} redox reaction was improved with Cr-doping. The first cycle discharge performances of $LiFe_{0.95}Cr_{0.05}PO_4/C$, at different current rates are presented in Fig. 9. The results are in good agreement with C-V recorded. Due to the limited lithium diffusion and electronic conduction, the discharge capacity decreases with increasing current rates but the capacity retention is appreciable. It can be seen from Fig. 10 that more than 95 % of discharge capacity was preserved even after 50 cycles at all current densities. Though Cr doped and undoped samples contain almost the same graphitic domain, the effect of graphitic carbon on electrochemical properties is similar in both the cases. Hence, the excellent capacity retention was purely due to Cr^{3+} substitution since the porosity is almost the same in both samples. Park et al. [16] reported that there was a drastic decrease in specific capacity

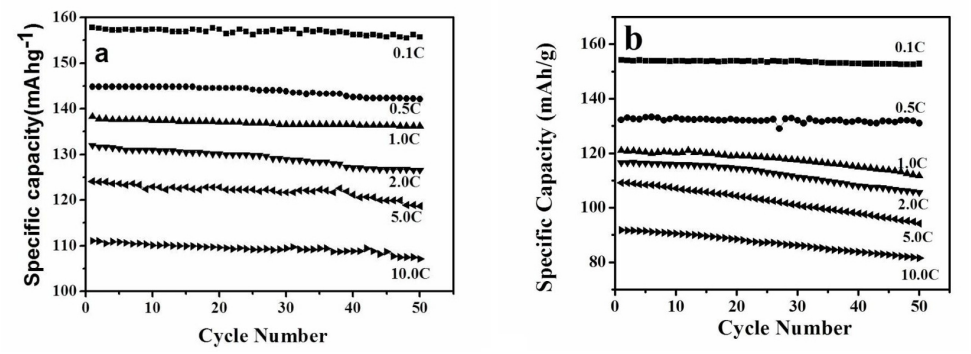

Fig. 10. Capacity per cycle of $LiFePO_4$/C and $LiFe_{0.95}Cr_{0.05}PO_4$/C at different current rates.

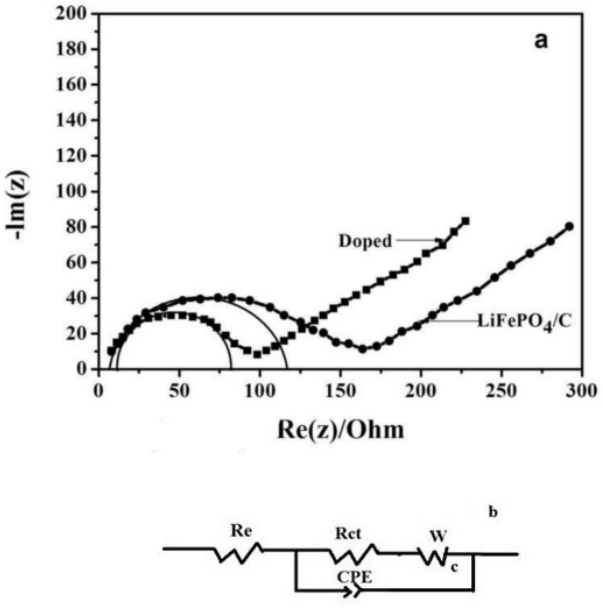

Fig. 11. (a) Electrochemical impedance spectra of the $LiFePO_4$/C and $LiFe_{0.95}Cr_{0.05}PO_4$/C cathodes (b) corresponding equivalent circuit model.

at current density less than 2 C. In our work, retention of capacity at lower current densities was attributed to the porosity, observed in the as prepared $LiFe_{0.95}Cr_{0.05}PO_4$/C, which can be seen in Fig. 3. The presence of pores increases the surface contact between an active material and electrolyte [20], which results in an increase in the diffusivity of Li^+ ions during charging/discharging cycles. The capacity retention at higher current densities can be attributed to both porosity and Cr^{3+} doping. Chromium causes an increase in the concentration of ionic vacancies [29] with accompanying conduction of electrons to maintain neutrality in the lattice of $LiFePO_4$ [30]. It accelerates the Li ion diffusivity which increases the kinetics of the phase transformation between heterosite (charged phase) and triphylite (discharged phase) during the charge-discharge cycles [31].

The kinetic processes of the $LiFePO_4$/C and $LiFe_{0.95}Cr_{0.05}PO_4$/C can be clearly depicted by EIS measurements. Impedance measurements were performed at room temperature on cells containing $LiFePO_4$/C or $LiFe_{0.95}Cr_{0.05}PO_4$/C as cathode material versus Li as anode in the voltage range of 2.0 to 4.1 V during the initial charge cycle, as shown in Fig. 11a. The figure depicts a simplified equivalent circuit model which was employed to analyze the impedance spectra, where the symbols, R_s, R_{ct}, and Z_w, denote the solution resistance, charge-transfer resistance and Warburg impedance, respectively. The intercept at the Z_{re} axis in high frequency range corresponds to the ohmic resistance (R_e), which represents the total electric resistance of the electrode material, the electrolyte resistance, and the resistance of the electric leads [32], respectively. The semicircle in the middle frequency range indicates the charge transfer resistance (R_{ct}). The inclined line in the low frequency range can be attributed to the Warburg impedance (Z_w), which is associated with lithium ion diffusion, in the $LiFePO_4$ particles [33]. Significant decrease in R_{ct} from 163.78 Ω in $LiFePO_4$/C to 98.42 Ω in $LiFe_{0.95}Cr_{0.05}PO_4$/C composite is found, which

indicates the enhancement of the charge-transfer reaction of the $LiFePO_4$/C with Cr^{3+} substitution, due to improvement in electron transportation.

4. Conclusions

Pristine and Cr substituted $LiFePO_4$ samples were successfully synthesized by solid-state reaction implementing microwave heating path. XRD and SEM investigations showed that the as-prepared composites were well crystallized in orthorhombic structure and the cell volume as well as the morphology varied on chromium doping. Compared to $LiFePO_4$/C, $LiFe_{0.99}Cr_{0.01}PO_4$/C composite showed the highest reversible capacity at different current densities, which can be attributed to the improvement in electric conductivity due to Cr^{3+} substitution. Taking into account all the analyses and results presented above, it can be concluded that the enhancement of chemical performance with Cr^{3+} substitution resulted in porosity, structure stability and ionic conductivities, which accelerated the Li^+ ion diffusion in the composites.

Acknowledgements

The research was supported by the Chinese National Science Foundation (51172175, 51072147) and the Hubei Science & Technology Plan (2012FFB05107, 2013BKB006).

References

[1] VENUGOPAL G., HUNT A., ALAMGIR F., *Mat. Matter.*, 5 (2010), 42.

[2] BRUCE P.G., SCROSATI B., TARASCON J.M., *Angew. Chem. Int. Edit.*, 47 (2008), 2930.

[3] PADHI A.K., NANJUNDASWAMY K.S., MASQUELIER C., GOODENOUGH J.B., *J. Electrochem. Soc.*, 14 (1997), 2581.

[4] WHITTINGHAM M.S., SONG Y., LUTTA S., ANDERSON A.S., THOMAS J.O., *J. Power Sources*, 108 (2002), 8.

[5] ZAGHIB K., STRIEBEL K., GUELI A., SHIM J., ARMAND M., GAUTHIER M., *Electrochim. Acta*, 50 (2004), 263.

[6] YUN N.J., HA H.W., JEONG K.H., PARK H.Y., KIM K., *J. Power Sources*, 160 (2006), 1361.

[7] GABRISCH H., WILCOX J.D., DOEFF M.M., *Electrochem. Solid. St. Lett.*, 9 (7) (2006), A360.

[8] CHUNG S.Y., BLOKING J.T., CHIANG Y.M., *Nat. Mater.*, 1 (2002), 123.

[9] YAMADA A., CHUNG S.C., HINIKUMA K., *J. Electrochem. Soc.*, 148 (2001), A224.

[10] GIBOT P., CABANAS M.C., LAFFONT L., LEVASSEUR S., CARLACH P., HAMELET S., TARASCON J.M., MASQUELIER C., *Nat. Mater.*, 7 (2008), 741.

[11] ZAVALIJ P.Y., CHERNOVA N.A., *J. Mater. Chem.*, 15 (2005), 3362.

[12] XU X., WEN Z., GU Z., XU X., LIN Z., *Electrochem. Commun.*, 6 (2004), 1233.

[13] DELMAS C., VIALA J.C., OLAZCUAGA R., FLEM G.L., HAGENMULLER P., *Mater. Res. Bull.*, 16 (1981), 83.

[14] SIGARYOV S.E., *Mater. Sci. Eng. B-Adv.*, 13 (1992), 117.

[15] YING J.R., LEI M., JIANG C.Y., WAN C.R., HE X.M., LI J.J., WANG L., REN J.G., *J. Power Sources.*, 158 (2006), 543.

[16] PARK C.K., PARK S.B., SHIN H.C., CHO W.I., JANG H., *B. Korean Chem. Soc.*, 32 (1) (2011), 191.

[17] NAIK A., ZHOU J., GAO C., WANG L., *Electrochim. Acta*, 214 (2014), 215.

[18] FENG Y., *Mater. Chem. Phys.*, 121 (2010), 302.

[19] MI C.H., ZHANG X.G., ZHAO X.B., LI H.L., *Mater. Sci. Eng. B-Adv.*, 129 (2006), 8.

[20] DOMINKO R., GOUPIL J.M., BELE M., GABERSCEK M., REMSKAR M., HANZEL D., *J. Electrochem. Soc.*, 152 (2005), A858.

[21] XU J., CHEN G., XIE C., LI X., ZHOU Y., *Solid State Commun.*, 147 (2008), 44.

[22] BHUVANESWARI M.S., BRAMNIK N.N., ENSLING D., EHRENBERG H., JAEGERMANN W., *J. Power Sources*, 180 (2008), 553.

[23] LI B., CHEN Y., WANG H., LIANG W., LIU G., REN W., LI C., LIU Z., RAO G., JINC C., ZHANG Z., *Chem. Commun.*, 50 (2014),799.

[24] MARKEVICH E., SHARABI R., HAIKET O., *J. Power Sources*, 196 (2011), 6433.

[25] LU Z.G., LO M.F., CHENG C.Y., *J. Phys. Chem. C*, 112 (2008), 7069.

[26] PARK K.C., HAYASHI T., TOMIYASU H., DRESSELHAUS M.S., *J. Mater. Chem.*, 15 (2005), 407.

[27] PADHI A.K., NANJUNDASWAMY K.S., MASQUELIER C., GOODENOUGH J.B., *J. Electrochem. Soc.*, 144 (1997), 1188.

[28] WANG Y.Q., WANG J.L., YANG J., NULI Y., *Adv. Funct. Mater.*, 16 (2006), 2135.

[29] MEETHONG N., KAO Y.H., SPEAKMAN S.A., CHIANG Y.M., *Adv. Funct. Mater.*, 19 (2009), 1060.

[30] HAUFFE K., *Oxidation of Metals*, Plenum Press, New York, 1965.

[31] SHIN H.C., PARK S.B., JANG H., *Electrochim. Acta*, 53 (2008), 7946.

[32] GAO F., TANG Z.Y., *Electrochim. Acta*, 53 (2008), 5071.

[33] SHIN H.C., CHO W.I., JANG H., *Electrochim. Acta*, 52 (2006), 1472.

Received 2014-12-09
Accepted 2015-05-26